논문 98-7-6-01

결합형 유한요소-경계요소 기법을 활용한 PZT5 구형 수중 수파기 시뮬레이션

장순석

PZT5 spherical hydrophone simulation using a coupled FE-BE method

Soon Suck Jarng

Abstract

This paper describes the application of a coupled finite element-boundary element method to obtain the steady-state response of a hydrophone. The particular structure considered is a flooded piezoelectric spherical shell. The hydrophone is three-dimensionally simulated to transduce an incident plane acoustic pressure onto the outer surface of the sonar spherical shell to electrical potentials on inner and outer surfaces of the shell. The acoustic field formed from the scattered sound pressure is also simulated. And the displacement of the shell caused by the externally incident acoustic pressure is shown in temporal motion. The coupled FE-BE method is described in detail.

1. Introduction

Most of hydrophones have the structure of a thin shell sphere. It is because we usually want to have omnidirectivity in its pressure-sensitive characteristics. Because of its simple type of structure, the behaviour of the spherical hydrophone is well known in analysis. Even so, any numerical method for simulating the hydrophone is often required because the numerical method could be further extended to other complicated types of structure for better performance. Since a hydrophone is used in water, modelling of the hydrophone must satisfy both internal materialistic transduction and externally radiating condition. In these aspects the finite element method (FEM) and the boundary element method (BEM) is perhaps the most suitable numerical techniques for the solution. Both methods were developed for the numerical solution of partial differential equations (PDE) with boundary conditions. Since both methods solve the PDEs by numerically elemental integration, they are compatible each other and therefore they can be coupled together [1,2]

Different types of in-air piezoelectric transducers have been simulated by the FEM [3-5]. And also modified FEMs such as the mixed FE perturbation method [6] or the mixed FE plane-wave method [7] have been developed in order to simulate an array of transducers or composite sonar transducers. Further developments have been made so as to include the effects of infinite fluid loading on transducer surface. For example, Bossut et. al. [8] and Hamonic et. al. [9] used fluid finite elements as an extension to structural finite elements with the condition that outer boundary of the fluid elements represents

* 조선대학교 제어계측공학과 (Deptment of Control & Instrumentation, Chousun University)
<접수일자 : 1998년 8월 24일>

continued radiation. Others used 'infinite' fluid elements for infinite acoustic radiation [10,11]. The BEM is probably accepted as the most suitable method for the radiation problem because the BEM directly solves the Helmholtz PDE with the radiation condition [1,2].

The main aim of this paper is to develope a coupled FE-BEM program and to simulate the structural behaviour of the flooded piezoelectric spherical shell when the sonar shell is driven by external incident acoustic pressure. The directivity pattern of the scattered acoustic pressure is shown in temporal motion and compared with that of a rigid steel sphere.

2. Numerical Methods

2.1 Finite Element Method (FEM)

The following equation (1) is the integral formulation of the piezoelectric equations:

$$\begin{aligned} \{F\}+\{F_I\} &= [K_{uu}]\{a\}+[K_{u\phi}]\{\phi\} \\ &\quad -\omega^2[M]\{a\}+j\omega[R]\{a\} \qquad (1) \\ -\{Q\} &= [K_{\phi u}]\{a\}+[K_{\phi\phi}]\{\phi\} \end{aligned}$$

where

{F}	Applied Mechanical Force
$\{F_I\}$	Fluid Interaction Force
{Q}	Applied Electrical Charge
{a}	Elastic Displacement
{ϕ}	Electric Potential
$[K_{uu}]$	Elastic Stiffness Matrix
$[K_{u\phi}]$	Piezoelectric Stiffness Matrix
	$[K_{\phi u}] = [K_{u\phi}]'$
$[K_{\phi\phi}]$	Permittivity Matrix
[M]	Mass Matrix
[R]	Dissipation Matrix
ω	Angular Frequency

The isoparametric formulation for 3-dimensional structural elements is well documented by Allik H. et. al. [3]. Each 3-dimensional finite element is composed of 20 quadratic nodes and each node has nodal displacement (a_x, a_y, a_z) and electric potential (ϕ) variables (Fig. 1). In local coordinates the finite element has 6 surface planes (±xy, ±yz, ±zx) which may be exposed to external fluid environment. The exposed surface is used as a boundary element which is composed of 8 quadratic nodes.

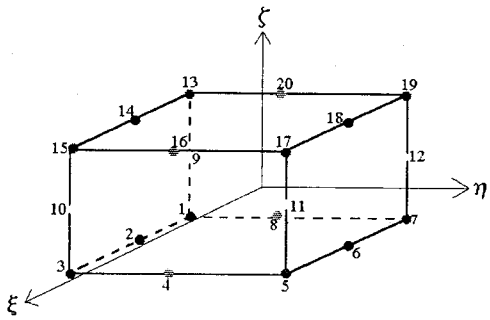

Figure 1 Each finite element is composed of 20 quadratic nodes. Each surface boundary has 8 quadratic nodes.

2.2 Boundary Element Method (BEM)

For sinusoidal steady-state problems, the Helmholtz equation, $\nabla^2\Psi + k^2\Psi = 0$, represents the fluid mechanics. Ψ is the acoustic pressure with time variation, $e^{j\omega t}$, and k(=ω/c) is the wave number. In order to solve the Helmholtz equation in an infinite fluid media, a solution to the equation must not only satisfy structural surface boundary condition (BC), $\frac{\partial \Psi}{\partial n} = \rho_f \omega^2 a_n$, but also the radiation condition at infinity, $\lim_{|r|\to\infty} \oint_S (\frac{\partial \Psi}{\partial r} + jk\Psi)^2 dS = 0$. $\frac{\partial}{\partial n}$ represents differentiation along the outward normal to the boundary. ρ_f and a_n are the fluid density and the normal displacement on the structural surface. The Helmholtz integral equations derived from Green's second theorem provides such a solution for radiating pressure waves;

$$\oint_S \left(\Psi(q) \frac{\partial G_k(p,q)}{\partial n_q} - G_k(p,q) \frac{\partial \Psi(q)}{\partial n_q} \right) dS_q = \beta(p)\ \Psi(p) - \Psi_{inc}(p) \tag{2}$$

where $G_k(p,q) = \frac{e^{-jkr}}{4\pi r}$, $r = |p-q|$

p is any point in either the interior or the exterior and q is the surface point of integration. β(p) is the exterior solid angle at p.

The acoustic pressure for the i^{th} global node, $\Psi(p_i)$, is expressed in discrete form [12]:

$$(\ 1 \le i \le ng\ )$$

$$\beta(p_i)\ \Psi(p_i) - \Psi_{inc}(p_i) =$$

$$= \oint_S \left(\Psi(q) \frac{\partial G_k(p_i,q)}{\partial n_q} - G_k(p_i,q) \frac{\partial \Psi(q)}{\partial n_q} \right) dS_q \tag{3a}$$

$$= \sum_{m=1}^{nt} \int_{S_m} \left(\Psi(q) \frac{\partial G(p_i,q)}{\partial n_q} - G(p_i,q) \frac{\partial \Psi(q)}{\partial n_q} \right) dS_q \quad q \in S_m \tag{3b}$$

$$= \sum_{m=1}^{nt} \int_{S_m} \left(\sum_{j=1}^{8} N_j(q)\ \Psi_{m,j} \frac{\partial G(p_i,q)}{\partial n_q} - G(p_i,q) \sum_{j=1}^{8} N_j(q) \frac{\partial \Psi_{m,j}}{\partial n_q} \right) dS_q \tag{3c}$$

$$= \sum_{m=1}^{nt} \sum_{j=1}^{8} \left(\int_{S_m} N_j(q) \frac{\partial G(p_i,q)}{\partial n_q} dS_q \right) \Psi_{m,j} - \rho_f\ \omega^2 \sum_{m=1}^{nt} \sum_{j=1}^{8} \left(\int_{S_m} N_j(q)\ G(p_i,q)\ n_q dS_q \right) a_{m,j} \tag{3d}$$

$$= \sum_{m=1}^{nt} \sum_{j=1}^{8} A^i_{m,j} \Psi_{m,j} - \rho_f\ \omega^2 \sum_{m=1}^{nt} \sum_{j=1}^{8} B^i_{m,j} a_{m,j} \tag{3e}$$

where nt is the total number of surface elements and $a_{m,j}$ are three dimensional displacements. Equation (3b) is derived from equation (3a) by discretizing integral surface. And equation (3c) is derived from equation (3b) since an acoustic pressure on an integral surface is interpolated from adjacent 8 quadratic nodal acoustic pressures corresponding the integral surface. Then equation (3d) is derived from equation (3c) by swapping integral notations with summing notations. Finally the parentheses of equation (3d) is expressed by upper capital notations for simplicity.

When equation (3e) is globally assembled, the discrete Helmholtz equation can be represented as

$$([A] - \beta[I])\{\Psi\} = +\rho_f\ \omega^2 [B]\{a\} - \{\Psi_{inc}\} \tag{4}$$

where [A] and [B] are square matrices of (ng by ng) size. ng is the total number of surface nodes.

Where the impedance matrices of equation (4), [A] and [B], are computed, two types of singularity arise [13]. One is that the Green's function of the equation, $G_k(p_i,q)$, becomes infinite as q approaches to p_i. This problem is solved by mapping such rectangular local coordinates into triangular local coordinates and again into polar local coordinates [14]. The other is that at certain wave numbers the matrices become ill-conditioned. These wave numbers are corresponding to eigenvalues of the interior Dirichlet problem [15]. One approach to overcome the matrix singularity is that [A] and [B] of equation (4) are modified to provide a unique solution for the entire frequency range [16-19]. The modified matrix equation referred to as the modified Helmholtz gradient formulation (HGF) [19] is obtained by adding a multiple of an extra integral equation to equation (4).

$$([A] - \beta[I] \oplus \alpha[C])\{\Psi\} = +\rho_f\ \omega^2 ([B] \oplus \alpha[D])\{a\} - (\Psi_{inc} \oplus \alpha \frac{\partial \Psi_{inc}}{\partial n_p}) \tag{5}$$

where

$$\alpha = \frac{-\sqrt{-1}}{k \cdot (Number\ of\ surface\ elements\ adjacent\ a\ surface\ node)}$$

[C] and [D] are rectangular matrices of (nt by ng) size. nt is the total number of surface elements. $\oplus$ symbol indicates that the rows of [C],[D] corresponding to surface elements adjacent a surface node are added to the row of [A],[B] corresponding to the surface node, that is,

$$\sum_{i=1}^{ng}\sum_{j=1}^{ng} A(i,j) = \sum_{i=1}^{ng}\sum_{j=1}^{ng} A(i,j) + \sum_{i=1}^{ng}\sum_{j=1}^{ng}\left(\sum_{m=1}^{S(i)} \alpha\ C(m,j)\right)$$

$$\sum_{i=1}^{ng}\sum_{j=1}^{ng} B(i,j) = \sum_{i=1}^{ng}\sum_{j=1}^{ng} B(i,j) + \sum_{i=1}^{ng}\sum_{j=1}^{ng}\left(\sum_{m=1}^{S(i)} \alpha\ D(m,j)\right) \quad (6)$$

where S(i) is the number of surface element adjacent a surface node. The derivation of the extra matrices [C],[D] are well described by Francis D.T.I.[19]. Equation (6) may be reduced in its formulation using superscript $\oplus$ for convenience;

$$A^{\oplus}\{\Psi\} = +\rho_f \omega^2 B^{\oplus}\{a\} - \Psi^{\oplus}_{inc} \quad (7)$$

where

$$([A]-\beta[I]\oplus\alpha[C]) \equiv A^{\oplus}$$

$$([B]\oplus\alpha[D]) \equiv B^{\oplus}$$

$$\left(\Psi_{inc}\oplus\alpha\frac{\partial\Psi_{inc}}{\partial n_p}\right) \equiv \Psi^{\oplus}_{inc}$$

Equation (7) can be written as

$$\{\Psi\} = +\rho_f \omega^2 (A^{\oplus})^{-1} B^{\oplus}\{a\} - (A^{\oplus})^{-1}\Psi^{\oplus}_{inc} \quad (8)$$

2.3 Coupled FE-BE Method

The acoustic fluid loading on the solid-fluid interface generates interaction forces. These forces can be related to the surface pressures by a coupling matrix [L] [2,12];

$$\{F_l\} = -[L]\{\widehat{\Psi}\} \quad (9)$$

where $[L] = \int N^t n N dS$. N is a matrix of surface shape functions and n is an outward normal vector at the surface element. N^t is the transposed form of N matrixss.

Equations (8) and (9) indicate that the interaction force can be expressed by functions of elastic displacement instead of acoustic pressure. This relationship can be applied to equation (1) when the sonar transducer model is submerged into the infinite fluid media:

$$\{F\} + [L](A^{\oplus})^{-1}\Psi^{\oplus}_{inc} = [K_{uu}]\{a\} + [\rho_f \omega^2 [L](A^{\oplus})^{-1}B^{\oplus}]\{a\} + [K_{u\phi}]\{\phi\} - \omega^2[M]\{a\} + j\omega[R]\{a\}$$

$$-\{Q\} = [K_{\phi u}]\{a\} + [K_{\phi\phi}]\{\phi\} \quad (10)$$

Since the present sonar transducer is modelled as a hydrophone, the internal force vector, {F}, and the applied electrical charge vector, {Q}, of equation (10) are removed. The only applied BC for the equation is external incident pressure, $[L](A^{\oplus})^{-1}\Psi^{\oplus}_{inc}$. The acoustic pressure in the far field is determined by $\beta(p)=1$ for given values of surface nodal pressure and surface nodal displacement;

$$\Psi(p_i) = \sum_{m=1}^{nt}\sum_{j=1}^{8} A^i_{m,j}\Psi_{m,j} - \rho_f \omega^2 \sum_{m=1}^{nt}\sum_{j=1}^{8} B^i_{m,j} a_{m,j} - (A^{\oplus})^{-1}\Psi^{\oplus}_{inc} \quad (11)$$

3. Results

The coupled FE-BE method has been programmed with Fortran language running at a supercomputer Cray C90. Calculation is done with double precision and the program is made for three dimensional structures. Because each structural node has 4 DOF, the size of the globally assembled coefficient matrices of the matrix equation are 4*ng by 4*ng. The particular structure considered is a flooded

piezoelectric (PZT5) spherical shell. Fig. 2 shows a part of the whole shell. The inner and the outer radii of the shell are 3.5cm and 4cm, respectively. The shell has been divided into 128 isoparametric elements. The figure shows only 8 elements as a slide which are rotationally symmetrical to z-axis. Global node numbers are attributed at 20 nodes of each element. It is desired to have more elements representing smaller local regions for higher frequency analysis. However, calculation with more number of nodes cost more time. Therefore meshing of elements depends on the maximal limit of interest frequency.

Table 1 shows the material properties of the PZT5 piezoelectric ceramic. The actual ceramic shell is radially polarized and therefore the electrode is coated radially on inner and outer surfaces. Hence, the axially polarized property values of Table 1 is to be converted to its radial polling direction by the tensor theory [20].

Table 1. Material Properties of PZT5 (Axially Polarized Properties, Dielectric coefficients at 100 KHz)

		Unit			Unit
ρ	7700	Kg/m^3	C_{xy}^{xy}	2.1053E+10 -i2.8063E+8	N/m^2
C_x^x	1.2035E+11 -i1.6042E+9	N/m^2	$e_{p,z}^x$	-5.3512	$(N/m^2)/(V/m)$
C_y^x	7.5179E+10 -i1.0021E+9	N/m^2	$e_{p,z}^y$	-5.3512	$(N/m^2)/(V/m)$
C_z^x	7.5090E+10 -i1.0021E+9	N/m^2	$e_{p,z}^z$	15.783	$(N/m^2)/(V/m)$
C_y^y	1.2035E+11 -i1.6042E+9	N/m^2	$e_{p,z}^{yz}$	6.9474	$(N/m^2)/(V/m)$
C_z^y	7.5090E+10 -i1.0010E+9	N/m^2	$e_{p,z}^{zx}$	6.9474	$(N/m^2)/(V/m)$
C_z^z	1.1087E+11 -i1.4779E+9	N/m^2	ε_x^x	7.7175E-9 +i1.5435E-10	F/m
C_{yz}^{yz}	2.1053E+10 -i2.8063E+8	N/m^2	ε_y^y	7.7175E-9 +i1.5435E-10	F/m
C_{zx}^{zx}	2.1053E+10 -i2.8063E+8	N/m^2	ε_z^z	6.9930E-9 +i1.3986E-10	F/m

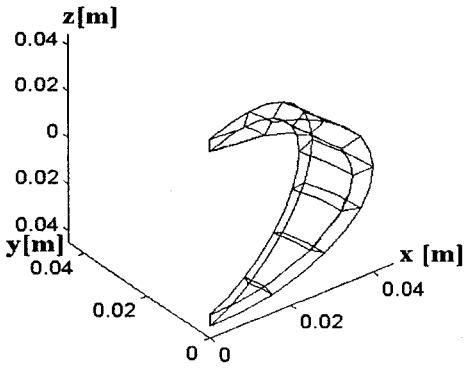

Figure 2 A structure is discretized into finite structural elements. A piezoelectric shell can be divided into either 128 elements.

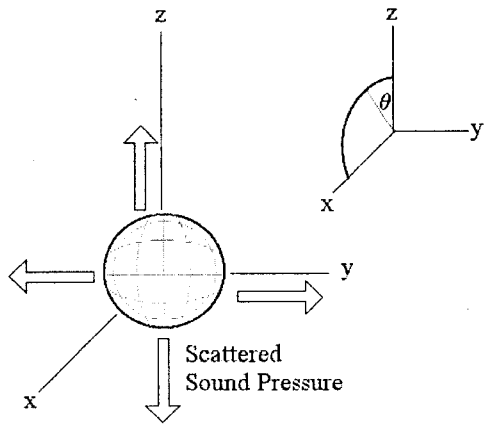

Figure 3 The acoustic pressure in the far field is calculated along the circle with the directivity angle θ.

The present modelling of the SONAR transducer is a pressure sensitive hydrophone. So, the hydrophone is three-dimensionally simulated to transduce an incident plane acoustic pressure onto the outer surface of the sonar spherical shell to electrical potentials on inner and outer surfaces of the shell. This acoustical energy drives the piezoelectric shell as a receiver. The incident acoustic pressure is of course scattered forwardly and backwardly after it is struck on the outer surface of the shell sphere. From equation (11) the

acoustic pressure in the far field is calculated around the circle with the directivity angle θ (Fig. 3). After normalizing the far field pressure, the averaged value of the pressure is calculated. This normalized and averaged value of the far filed pressure is then used as the quantitative degree of the omnidirectional directivity.

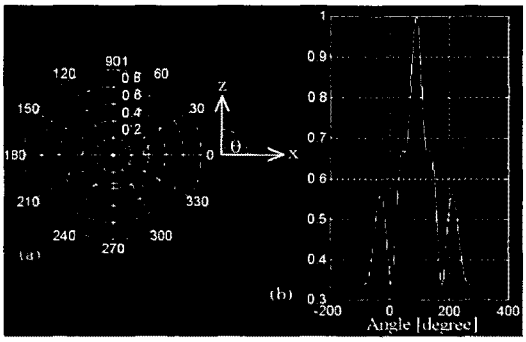

Figure 4 Normalized directivity pattern of scattered acoustic press of a solid steel sphere (a) In polar form (b) In rectangular form, IR=0cm, OR=4cm, 128 elements, ka=π.

Fig. 4 shows the directivity pattern of a solid steel sphere in polar form (a) and in rectangular form (b) for 18515.0 Hz input frequency which is equivalent to ka=π (a is radius (4cm)). This particular figure is often used to confirm the calculation of the coupled FE-BEM algorithm to be correct [21]. Fig. 5 shows the directivity patterns of the PZT5 spherical shell for the same ka=π. The inner and outer surfaces of the PZT5 shell has been electroded. The electroding of the PZT5 shell is simply done by manipulating the global coefficient matrix [21]. The potential difference between inner and outer surfaces of the excited PZT5 shell is 0.652 [mV] in magnitude at 18515.0 Hz. This potential difference value is in fact the same as hydrophone sensitivity because the amplitude of the incident plane pressure wave was 1 [Pa]. Theoretical sensitivity value of the present shell-typed hydrophone is about 0.412 [mV] below 27593Hz resonant frequency [22]. Fig. 6 shows the frequency response of the hydrophone sensitivity.

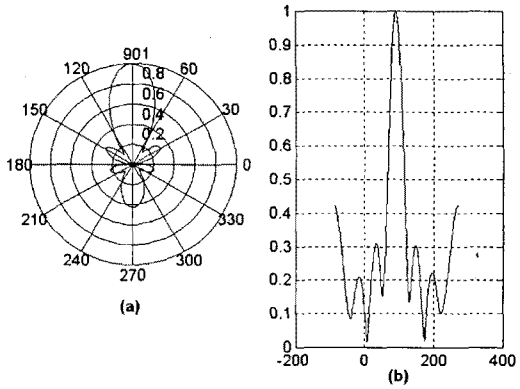

Figure 5 Normalized directivity pattern of scattered acoustic press of a PZT5 spherical shell (a) In polar form (b) In rectangular form. The inner and outer surfaces of the ceramic shell are electroded for equipotential surfaces respectively.

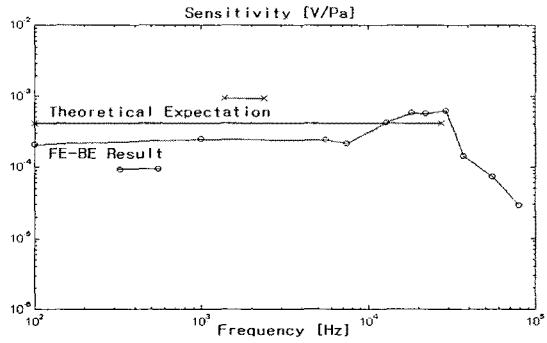

Figure 6 Simulated frequency response of hydrophone sensitivity.

Fig. 7 shows the surface acoustic pressure on the outer surface of the PZT5 shell at a particular instant phase. Since the present hydrophone simulation is calculated for steady-state frequency response, its temporal deformation could be figured with different phases. In the figure, the three dimensional displacement has been exaggerated to emphasize the form of vibration. And Fig. 8 shows the temporal moving picture of the PZT5 shell for different phases. The input frequency is 18515.0 Hz.

And Fig. 9 shows directivity patterns of the spherical shell hydrophone at different frequencies. The figure shows how directivity pattern is changed with different frequencies.

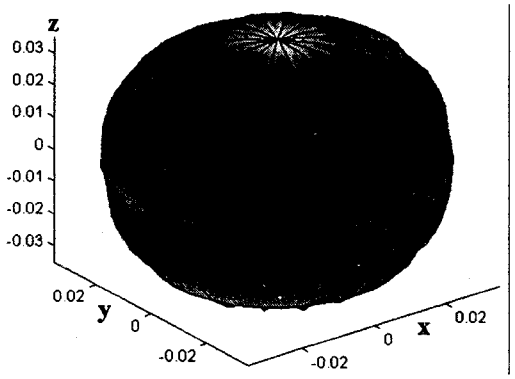

Figure 7 Three dimensional displacement of the PZT5 shpere at a constant phase. The degree of the gray color intensity indicates the surface pressure on the sphere at 18515Hz.

The surface acoustic pressure on the outer surface of the PZT5 shell at a particular instant phase. The three dimensional displacement has been exaggerated to emphasize the form of vibration. ka=π

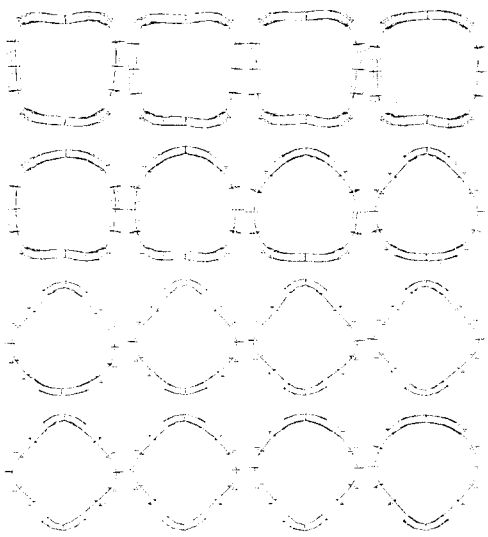

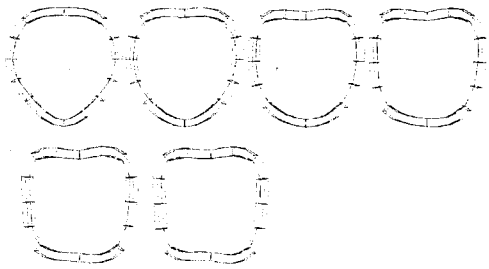

Figure 8 Vibrational Modes (at 18515.0 Hz) for different phases.

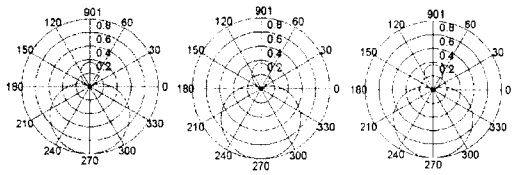

(a) 185.15 Hz (ka=0.01π) (b) 555.45 Hz (ka=0.03π) (c) 925.75 Hz (ka=0.05π)

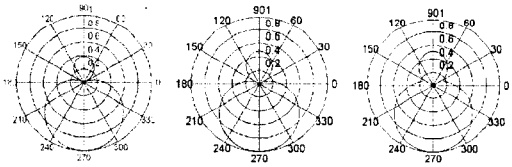

(d) 1851.5 Hz (ka=0.1π) (e) 4628.75 Hz (ka=0.2π) (f) 6480.25 Hz (ka=0.35π)

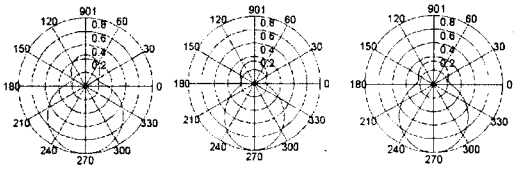

(g) 7406.0 Hz (ka=0.4π) (h) 8794.6 Hz (ka=0.475π) (i) 8331.8 Hz (ka=0.45π)

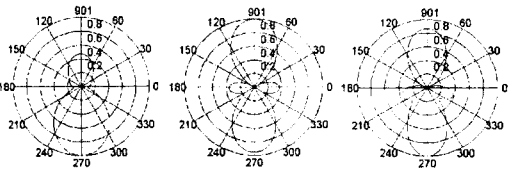

(j) 9257.5 Hz (ka=0.5π) (k) 11109 Hz (ka=0.6π) (l) 12960.5 Hz (ka=0.7π)

A

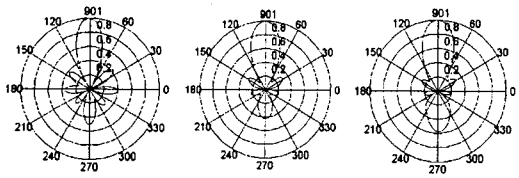

(m) 16663.5 Hz (ka=0.9π) (n) 18515 Hz (ka=π) (o) 19966.1 Hz (ka=1.1π)

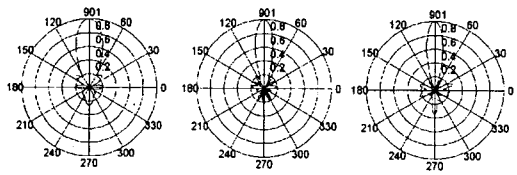

(p) 23144 Hz (ka=1.25π) (q) 37030 Hz (ka=2π) (r) 46288 Hz (ka=2.5π)

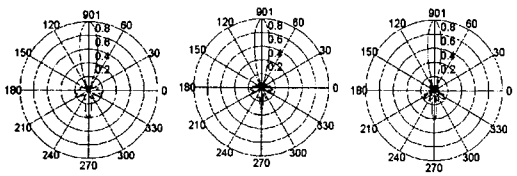

(s) 50916 Hz (ka=2.75π) (t) 55545 Hz (ka=3π) (u) 74060 Hz (ka=4π)

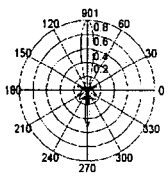

(v) 92575 Hz (ka=5π)

Figure 9 Directivity patterns at different frequencies.

4. Conclusion

A coupled FE-BE method has been developed and applied to simulate a sonar transducer. The particular structure considered is a flooded piezoelectric spherical shell. The transducer is three-dimensionally simulated to transduce an incident plane acoustic pressure onto the outer surface of the shell to electrical potentials on inner and outer surfaces of the shell. The acoustic field formed from the scattered sound pressure is also simulated. And the displacement of the shell caused by the externally incident acoustic pressure is shown in temporal motion. The coupled FE-BE method has been used for predicting the mechanical and the acoustical behaviour of the spherical shell-typed sonar transducer. The results of the directivity patterns of Fig. 9 show the variation of the beam pattern at different frequencies up to ka=5π.

In general, as the frequency of external loading to the piezoelectric transducer is increased, more number of structural finite elements are necessarily required. Most of executing time of the coupled FE-BEM program is spent in matrix solution in which the size of the matrix is increased to 4ng by 4ng matrix as the number of global nodes are increased to ng. Therefore the present numerical method need to be linked to a faster matrix solver such as parallel processing for next work.

ACKNOWLEDGMENTS

This study was supported by research funds from Chosun University, 1998

References

[1] R.R. Smith, J.T. Hunt and D. Barach, "Finite element analysis of acoustically radiating structures with application to sonar transducers", J. Acoust. Soc. Am. vol. 54, No. 5, PP:1277-1288, 1973.

[2] O.C. Zienkiewicz, D. Kelly and P. Bettess, "The coupling of finite element method and boundary solutions procedures", Int. J. Num. Methods Eng., Vol. 11, PP:355-375, 1977.

[3] H. Allik and T.J.R. Hughes, "Finite element method for piezoelectric vibration", Int. J. Numer. Method Eng., Vol. 2, PP:151-157, 1970.

[4] Y. Kagawa and T. Yamabuchi, "Finite element approach for a piezoelectric circular rod", IEEE Trans. Sonics & Ultrasonics, Vol. su-23, No. 6, PP:379-385, 1976.

[5] N.F. Ivina, "Numerical analysis of the normal

modes of circular piezoelectric plates of finite dimensions", Sov. Phys. Acoust., Vol. 35(4), PP:385-388, 1989.

[6] D. Boucher, M. Lagier and C. Maerfeld, "Computation of the vibrational modes for piezoelectric array transducers using a mixed finite element perturbation method", IEEE Trans. Sonics & Ultrasonics, Vol. su-28, No. 5, PP:318-330, 1981.

[7] J.N. Decarpigny, J.C. Debus, B. Tocquet and D. Boucher, "In-air analysis of piezoelectric tonpilz transducers in a wide frequency band using a mixed finite-plane wave method", J. Acoust. Soc. Am. Vol. 78, No. 5, PP:1499-1507, 1985.

[8] R. Bossut and J.N. Decarpigny, "Finite element modeling of radiating structures using dipolar damping elements", J. Acoust. Soc. Am. Vol. 86, No. 4, PP:1234-1244, 1989.

[9] B. Hamonic, J.C. Debus and J.N. Decarpigny, "Analysis of a radiating thin-shell sonar Transducer using the finite element method", J. Acoust. Soc. Am. Vol. 86, No. 4, PP:1245-1253, 1989.

[10] J.M.M.C. Marques and D.R.J. Owen, "Infinite elements in quasi-static materially nonlinear problems", Comp. & Struc., Vol. 18(4), PP:739-751, 1984.

[11] J.P.E. Goransson and C.F. Davidsson, "A three dimensional infinite element for wave propagation", J. Sound & Vibration, Vol. 115(3), PP:558-559, 1987.

[12] L.G. Copley, "Integral equation method for radiation from vibrating bodies", J. Acoust. Soc. Am. Vol. 41, PP:807-816, 1967.

[13] L.G. Copley, "Fundamental results concerning integral representations in acoustic radiation", J. Acoust. Soc. Am. Vol. 44, PP:28-32, 1968.

[14] E. Skudrzyk, "The foundation of acoustics", (Springer-Verlag, New York, 1971), PP:408-409, Equation(76), 1971.

[15] D.T.I. Francis, "A boundary element method for the analysis of the acoustic field in three dimensional fluid-structure interaction problems", Proc. Inst. of Acoust., Vol. 12, Part 4, PP:76-84, 1990.

[16] H.A. Schenck, "Improved integral formulation for acoustic radiation problems", J. Acoust. Soc. Am. Vol. 44, PP:41-58, 1968.

[17] A.J. Burton and G.F. Miller, "The application of integral integration methods to the numerical solutions of some exterior boundary problems", Proc. R. Soc. London, Ser. A 323, PP:201-210, 1971.

[18] R.F. Kleinman and G.F. Roach, "Boundary integral equations for the three dimensional Helmholtz equation", SIAM Rev., Vol. 16, PP:214-236, 1974.

[19] D.T.I. Francis, "A gradient formulation of the Helmholtz integral equation for acoustic radiation and scattering", J. Acoust. Soc. Am. Vol. 93(4) Part 1, PP:1700-1709, 1993.

[20] W.P. Mason, "Electromechanical transducer and wave filters", D.Van Nostrand Co. Inc., 2nd ed., New York, 1948.

[21] S.S. Jarng, "Sonar transducer analysis using a coupled FE-BE method", Proc. of the 12 Korea Automatic Control Conf., Inst. of Control & System Eng. Korea, Vol. 12, PP:1750-1753, 1997.

[22] D. Stansfield, "Underwater Electroacoustic Transducers", Published by Bath University and Institute of Acoustics, PP:297-300, 1990.

著 者 紹 介

장순석(張淳晳)(Soon Suck Jarng)
1961년 12월 11일생, 1984년 2월: 한양대학교 전자공학과 졸업(공학사), 1985년 9월:영국 헐대학교 전자공학과 졸업(공학석사), 1988년 9월:영국 버밍험대학교 의과대학 생리학과 졸업(이학석사), 1991년 12월:영국 버밍험대학교 전기전자공학과 졸업(공학박사), 1992년 3월~현재:조선대학교 제어계측공학과 부교수

※ 주관심분야: 수중음향, 지중음향, 유한요소-경계요소 기법, 압전센서, 달팽이관 필터 등